Analysis of the time-domain spectrum of hydrogen in electric field near helium surface

Xiaoqing Gong (龚晓青) and Guangcan Yang (杨光参)*

School of Physics and Electronic Information Engineering, Wenzhou University, Wenzhou 325035, China

**Corresponding author: yanggc@wzu.edu.cn*

Received October 26, 2010; accepted December 7, 2010; posted online March 28, 2011

The Ryderberg electronic wave packet dynamics of hydrogen atom near helium surface in an electric field is investigated using the semiclassical method. The autocorrelation function is calculated when the photoionized electron is excited by a short laser pulse for different atom-surface separations. The results show that new recurrences appear because of the helium surface, and the number of recurrent peaks increases with the decrease in atom-surface distance. The new feature is ascribed to the bifurcation of new closed orbits in the classical dynamics of the photoionized electron. Therefore, surface properties have a significant effect on the spectrum of nearby atoms or ions.

OCIS codes: 020.0020, 020.1670, 300.6500, 350.6670.

doi: 10.3788/COL201109.040202.

In recent decades, short-pulse laser technology has been developed, and one of its applications is the generation of electronic wave packets for examining their evolution in atomic systems[1−5]. The Rydberg wave packet is an interesting model for studying the correspondence between quantum and classical mechanics. This packet has been proven to travel like a classical particle along the classical orbit within a short time, but it exhibits quantum behavior within a long time[6].

Recently, the autocorrelation function of the Rydberg H atom in an external field has been studied using the closed-orbit theory[7−9]. The autocorrelation functions of the Rydberg H atom in magnetic and strong electric fields have been investigated intensively[5]. In our previous work, the photodetachment and time-resolved photodetached spectroscopy of H^- in an electric field near an elastic surface was examined[4,10−12]. In 2004, Zhang *et al.* obtained improved values for the dissociation energies of molecular hydrogen and its ion using a high-resolution pulse-amplified laser to probe the second dissociation limit[13]. Recently, Wang examined the wave packet dynamics of the photodetachment of H^- near an dielectric surface[14]. With regard to the time-domain spectrum of hydrogen in an electric field near helium surface, however, no analysis has been done to date to our knowledge. Therefore, we examine the autocorrelation function of the Rydberg H atom in an electric field near helium surface. A short-pulse laser is used to stimulate the H atom in an electric field near helium surface. Using the closed-orbit theory, the autocorrelation function of the H Rydberg wave packet corresponding to different atom-surface distances is calculated.

The H atom nucleus is assumed to be positioned at the origin of the coordinate system. The elastic surface is fixed in the $z = -d$ plane, where d is the distance between the atom and the elastic surface. The electric field is perpendicular to the elastic surface along the z-axis positive direction. The problem has cylindrical symmetry, so cylindrical coordinates (ρ, z, ϕ) are used. The Hamiltonian of a hydrogen atom in a homogeneous static electric field F is[15]

$$H = \frac{1}{2}\left(p_z^2 + p_\rho^2 + l_z^2/\rho^2\right) - 1/\left(\rho^2 + z^2\right)^{1/2} + Fz. \quad (1)$$

By adopting a scaled-variables method and semiparabolic coordinates (u, v), and then considering the case of $l_z = 0$, the transformed Hamiltonian is defined as

$$\widetilde{H} = \frac{1}{2}\left(p_u^2 + p_v^2\right) + \frac{1}{2}\left(u^4 - v^4\right) - \varepsilon\left(u^2 + v^2\right) - 2, \quad (2)$$

where $P_u = \mathrm{d}u/\mathrm{d}\tau, p_v = \mathrm{d}v/\mathrm{d}\tau$, and $\varepsilon = E/F^{1/2}$ is the scaled energy. After this transformation, the Coulomb singularities are eliminated.

The above analysis does not consider an elastic surface. In fact, there is no interaction between the electron and the elastic surface unless the electron reaches the elastic surface. When the electron does, it returns. To understand better the nature of the problem, their interaction is dealt with as a fully elastic collision. Using fully elastic collision, the formula can be written as

$$p_u = p'_u, p_v = -p'_v, \quad (3)$$

where p_u, p_v and p'_u, p'_v are the momenta before and after the collision. The above formula is the basic principle of the fully elastic collision model.

Therefore, the motion equations for (u, v, p_u, p_v) of Eq. (2) can be numerically integrated, namely,

$$\dot{u} = \frac{\partial \widetilde{H}}{\partial p_u}, \dot{v} = \frac{\partial \widetilde{H}}{\partial p_v}, \dot{p}_u = -\frac{\partial \widetilde{H}}{\partial u}, \dot{p}_v = -\frac{\partial \widetilde{H}}{\partial v}. \quad (4)$$

An independent variable τ is introduced, which connects to time $\hat{t}$ by[15]

$$\frac{\mathrm{d}\hat{t}}{\mathrm{d}\tau} = u^2 + v^2. \quad (5)$$

Using the standard fifth-order Runge-Kutta method to integrate the motion equations, all the closed orbits of the Rydberg hydrogen atom near an elastic surface along with a constant electric field with different atom-surface

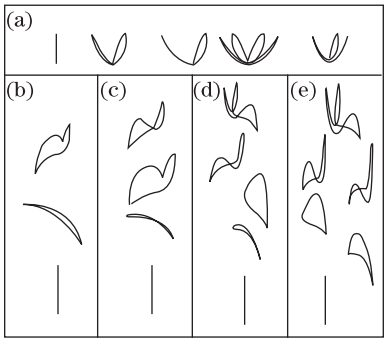

Fig. 1. Some closed orbits drawn in (ρ, z) space. (a) Five orbits with the atom-surface distance $d = \infty$; (a)+(b) eight orbits with $d = 2000$ a.u.; (a)+(c) nine orbits with $d = 1500$ a.u. (a)+(d) ten orbits with $d = 1000$ a.u.; (a)+(e) eleven orbits with $d = 500$ a.u.

distances are determined. In our calculation, $\varepsilon = -0.266$ and F=2000 V/cm; closed orbits with scaled actions smaller than 25 are used. Some closed orbits are shown in Fig. 1. For each closed orbit, its action S_k and scaled period T_k are calculated, where k runs over all of the closed orbits. These are shown in Table 1.

Table 1. Properties of the Electron of the H Atomic Systems at ε = –0.266 and F = 2000 V/cm, with the Scaled Action Less Than 25 and with Different Atom-Surface Distances

d^{a}	o^{b}	$\theta_{\mathrm{i}}^{\mathrm{c}}$	$S_{\mathrm{k}}^{\mathrm{d}}$	$T_{\mathrm{k}}^{\mathrm{e}}$
	1	0.00	446	2.26
	2	5.00	9.18	4.58
∞	3	13.00	13.52	7.33
	4	15.00	17.92	10.43
	5	15.23	22.42	13.35
	6	30.00	18.40	6.91
2000 a.u.	7	90.00	13.05	4.77
	8	180.00	8.01	1.88
	6	24.31	20.06	7.95
1500 a.u.	7	30.00	15.22	5.34
	8	90.00	11.89	2.49
	9	180.00	6.91	1.73
	6	17.00	20.23	7.97
	7	25.00	15.83	5.18
1000 a.u.	8	60.00	10.45	2.85
	9	90.00	10.14	2.40
	10	180.00	4.89	1.44
	6	17.00	19.02	7.89
	7	14.00	12.00	5.21
	8	25.00	14.73	5.12
500 a.u.	9	60.00	8.07	2.66
	10	90.00	8.63	2.31
	11	180.00	3.42	1.13

[a]The atom-surface distance of the H atomic systems; [b]number of orbits; [c]initial outgoing polar angle (in degrees) of the orbits; [d]scaled action; [e]period of closed orbits in units of picoseconds.

The autocorrelation function is an important quantity that can reflect the dynamic properties of the Rydberg wave packet and can be defined as[16]

$$\psi^{\mathrm{AC}}(t) = \langle\psi(0)|\psi(t)\rangle, \tag{6}$$

where $|\psi(t)\rangle$ is the wave function at time t. It shows that the overlap between the wave function at time t and the initial wave function $|\psi(0)\rangle$ is directly measured. The autocorrelation function to the system for the H atom near an elastic surface in an electric field is applied. The initial state of the atomic system is $\psi_{\mathrm{i}}(r)$. In the present case, the wave packet is produced by applying a short-pulse laser which is assumed to have the following form[16]:

$$f(t) = f_m \exp(-t^2/2\tau^2)\cos(wt + \phi), \tag{7}$$

where w, f_m, and τ are the frequency, peak amplitude, and pulse width, respectively. The system can be excited to state $\psi_{\mathrm{f}}(r)$ with energy E_{f} centered at $E_{\mathrm{f}}^{\mathrm{c}} = E_{\mathrm{i}} + w$ and with a few $1/\tau$ widths.

Applying the time-dependent perturbation theory and using the same method given in Ref. [16], the autocorrelation function can be written as

$$\langle\psi(0)|\psi(t)\rangle = \int \mathrm{d}E \mathrm{e}^{-\mathrm{i}Et}|g(E - E_{\mathrm{i}})|^2 \left[\frac{Df(E)}{2(E - E_{\mathrm{i}})}\right], \tag{8}$$

where

$$g(E_{\mathrm{f}} - E_{\mathrm{i}}) = \int \mathrm{d}t f(t)\mathrm{e}^{\mathrm{i}(E_{\mathrm{f}} - E_{\mathrm{i}})t} \tag{9}$$

is the Fourier transformation of the short-pulse laser, and $Df(E)$ is the oscillator-strength density. Adopting the rotating wave approximation,

$$g(E - E_{\mathrm{i}}) = A\tau\left(\frac{\pi}{2}\right)^{1/2} \mathrm{e}^{-(E - E_{\mathrm{i}} - w)^2\tau^2/2}\mathrm{e}^{\mathrm{i}\phi}. \tag{10}$$

As is known, $|g(E - E_{\mathrm{i}})|^2$ is a Gaussian shape with width $1/\tau$. It attains the peak when the energy $E_{\mathrm{f}}^{\mathrm{c}} = E_{\mathrm{i}} + w$, and its value diminishes quickly when E moves away from $E_{\mathrm{f}}^{\mathrm{c}}$ by more than a few $1/\tau$. Therefore, the effective part of Eq. (8) is confined to an interval centered at E_{f} and with $1/\tau$ width. According to the closed-orbit

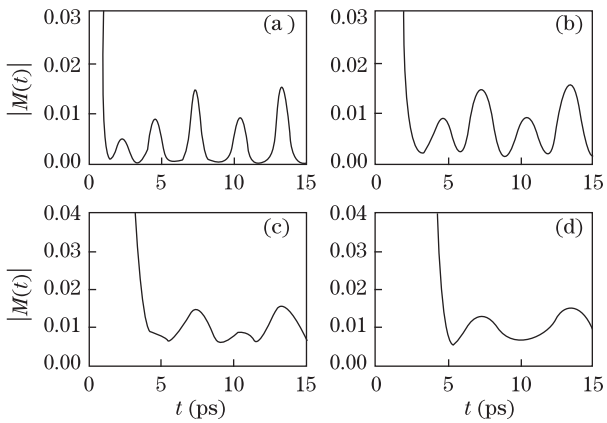

Fig. 2. Plots of the module of $M(t)$ of the H atom autocorrelation function at scaled energy $\varepsilon = -0.266$, and the electric field $F = 2000$ V/cm for different pulse widths with the atom-surface distance $d = \infty$. (a) $\tau = 0.2$ ps; (b) $\tau = 0.4$ ps; (c) $\tau = 0.8$ ps; (d) $\tau = 1.0$ ps.

theory[7−9], the oscillator-strength density can be approximated as

$$Df(E_{\rm f}^{\rm c}+\delta E)=Df_0(E_{\rm f}^{\rm c})+\sum_k C_k(E_{\rm f}^{\rm c})$$
$$\times\sin\left[T_k(E_{\rm f}^{\rm c})\delta E+\frac{1}{2}T_k'(E_{\rm f}^{\rm c})\delta E^2+\Delta_k(E_{\rm f}^{\rm c})\right], \quad (11)$$

where $T_k'(E_{\rm f}^{\rm c})=[{\rm d}T_k(E_{\rm f}^{\rm c})/{\rm d}E_{\rm f}^{\rm c})]$, δE is the deviation from $E_{\rm f}^{\rm c}$, and the sum is over all the closed orbits of the system. Equation (11) is an approximation of the more accurate expression of oscillator-strength density in the closed-orbit theory. Each oscillation in Eq. (11) corresponds to a closed orbit of the atomic system that leaves and finally returns to the nuclei. The oscillation is related to the stability property of the corresponding closed orbit, the laser polarization, and the initial quantum state.

Using Eqs. (11) and (10), in Eq. 8, replacing $(E-E_{\rm i})$ in the denominator of the integrand by w and carrying out the integral, we can obtain

$$\psi^{\rm AC}(t)=\left[\frac{\tau A^2\sqrt{\pi^3}(Df_0)}{4w}\right]$$
$$\times{\rm e}^{-{\rm i}E_{\rm f}^{\rm c}t}\{{\rm e}^{-t^2/4\tau^2}+\sum_k[C_k^-(t)+C_k^+(t)]\},$$
$$C_k^{\pm}=\left[\frac{C_k}{2(Df_0)\alpha_k^{\mp}}\right] \quad (12)$$
$$\times{\rm e}^{-[(t\mp T_k)^2/4\tau^2(\alpha_k^{\mp})^2]\pm{\rm i}(\Delta_k-\pi/2)}, \quad (13)$$

where $\alpha_k^{\pm}=\sqrt{1\pm{\rm i}[T_k'(E_f^c)/2\tau^2]}$. When T_k' approaches zero, $\alpha_k^{\pm}$ approaches 1. Equation (12) is the autocorrelation function involving the laser-pulse parameters and the dynamic variables in the closed-orbit theory. The details on parameters Df_0, C_k, and Δ_k can be found in Refs. [15, 17, 18]. From the above formulas, the autocorrelation function includes a sum of modified Gaussian terms. It shows that each modified Gaussian term in the autocorrelation function comes from a parent oscillation term in the oscillator-strength density expressed in the closed-orbit theory. Evidently, there is the following correspondence: the pair of terms with the same index k in the sum of Eq. (12) corresponds to the kth closed orbit, and the two terms are centered respectively at $t=T_k$ and $t=-T_k$. The term centered at $t=0$ in Eq. (12) comes from the background term in the oscillator-strength density and is not related to any real closed orbit.

If a short-pulse laser of the form in Eq. (7) is applied to H atom near an elastic surface along with a constant electric field, and the detached electron wave function is denoted by $\psi(t)$, the autocorrelation function can be written as

$$\langle\psi(0)|\psi(t)\rangle=C_0M(t), \quad (14)$$
$$M(t)={\rm e}^{-t^2/4\tau^2}+\sum_k[C_k^-(t)+C_k^+(t)], \quad (15)$$
$$C_0=\left[\frac{\tau A^2\sqrt{\pi^3}(Df_0)}{4w}\right]{\rm e}^{-{\rm i}E_{\rm f}^{\rm c}t}. \quad (16)$$

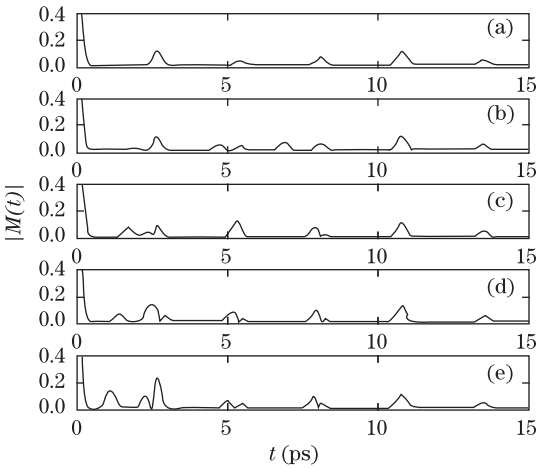

Fig. 3. Comparison of the module of $M(t)$ of the H atom autocorrelation functions at scaled energy $\varepsilon=-0.266$ and electric field $F=2000$ V/cm; $\tau=0.1$ ps. (a) Five peaks with the atom-surface distance $d=\infty$; (b) eight peaks with $d=2000$ a.u.; (c) eight peaks with $d=1500$ a.u.;(d) nine peaks with $d=1000$ a.u.; (e) nine peaks with $d=500$ a.u.

As shown in Eq. (15), the autocorrelation function of the Rydberg H atom in an electric field near an elastic surface contains $(2k+1)$ peaks centered at $t=0$ and $\pm T_k$. The peak centered at $t=0$ comes from the non-oscillatory background term in the oscillator-strength density in Eq. (11). The other peaks centered at $t=\pm T_k$ are related to the oscillatory terms in the oscillator-strength density in Eq. (11). In a comparison of Eqs. (14) and (15), $M(t)$ can be regarded as an effective autocorrelation function because the constant factor C_0 has no influence on the experimental measurement.

By integrating Hamiltonian motion Eq. (4), some of the closed orbits of the Rydberg H atom in an electric field near an elastic surface with the different atom-surface distances d are determined. On this basis, the autocorrelation function of H atom in an electric field near an elastic surface with the atom-surface distance d is calculated. The time dependence of the absolute value of the autocorrelation function is entirely included in the function $|M(t)|$, which is shown in Fig. 2 for positive time. Due to symmetry $|M(t)|=|M(-t)|$, the negative time part can be obtained. In Figs. 2(a)–(d), the autocorrelations at four different widths of the pulse with the atom-surface distance $d=\infty$ are shown. In the figure, the peak is centered at $t=0$ from the background item in the oscillator-strength density and is unrelated to any real orbit. From Fig. 2(a), there are five other peaks centered at $T=T_1$, T_2, T_3, T_4, T_5 which correspond to five orbits. Figure 2(b) shows the interference with only four peaks appearing. Figures 2(c) and (d) show the interference with only two or three peaks appearing.

From the figure, when the width of the laser pulse becomes longer, the oscillations become smoother. This phenomenon can be explained as follows. The electronic wave packet produced by a narrower laser pulse is more localized in space, and distinguishing those belonging to different closed orbits is easy. As the laser pulse width increases, distinguishing the packets becomes difficult due to their space expansion and the interference between them. Due to this effect, the width of peaks in the au-

tocorrelation function increases, and even two adjacent peaks merge into one.

As the atom-surface distance d becomes infinite, that is, the surface is not located, the interaction between the atom and the elastic surface becomes very weak. Therefore, the influence of elastic collision can be neglected. In this case, the number of closed orbits is the least, which is only five. With a decrease in atom-surface distance d, the influence of elastic collision becomes significant so that the number of closed orbits increases. For example, when the distance $d = 2000$ a.u., 8 closed orbits are found. When $d = 1500$ a.u., 9 closed orbits are found. As d is reduced to 1000 a.u., 10 closed orbits are found. When $d = 500$ a.u., 11 closed orbits are found. The information on some of the orbits is shown in Table 1.

The absolute value of $M(t)$ is a set of δ-like functions shown as the peaks in Fig. 3. The recurrent peaks are centered at T_k , which corresponds to a specific closed orbit of the photoionized electron. When the atom-surface distance d is fixed, there is a series of recurrent peaks in the corresponding autocorrelation function of the photoionized electron. Figure 3 shows the autocorrelation functions at different distances, where several plots are placed together in overlay form. New recurrent peaks are created due to the bifurcation of new orbits from the existing orbits with decreasing distance d. Figures 3(a)–(e) show the autocorrelation functions with five different atom-surface distances d at a fixed laser pulse width τ=0.1 ps. Among them, the peak centered at $t = 0$ comes from the background term, which does not belong to any closed orbit. Figure 3(a) corresponds to the case of free space. Five discrete recurrent peaks corresponding to the basic closed orbits are shown in Fig. 1(a), which is attributed to the large differences between the adjacent orbits. Figure 3(b) shows the case when the atom-surface distance $d = 2000$ a.u., where eight recurrent peaks can be found. Aside from the contribution of the basic orbits in Fig. 1(a), the new peaks correspond to the newly created closed orbits shown in Fig. 1(b). Figure 3(c) also shows eight peaks in the autocorrelation function with the atom-surface distance $d = 1500$ a.u., but there are 9 closed orbits as shown in Fig. 1(c). This phenomenon occurs because the recurrent periods of two orbits are very close to contribute a common recurrence. Figures 3(d) and (e) show the cases of closer distances $d = 1000$ and 500 a.u., respectively. The same phenomenon of common recurrence exists in both cases, resulting in more than one closed orbits contributing to one recurrent peak. The height and width of the recurrent peak increase although the number of peaks is reduced. However, with an increase in the number of orbits, distinguishing them is difficult because of their expansion in space and the superposition between them. Generally, there are less closed orbits in the system, and the periods of neighboring orbits are significantly different when the surface is far away from the atom. The recurrent peaks in the correlation function peaks emerge distinctly, and the corresponding closed orbits can easily be identified. When the atom approaches the surface, more and more closed orbits are bifurcated, and the electronic returning periods of some orbits are very close, with some adjacent peaks in the autocorrelation function merging into one to create a wider and higher recurrent peak.

In conclusion, the dynamics of the Rydberg H atom near a helium surface with different atom-surface distances in a perpendicular electric field is examined. By applying the closed-orbit theory, the autocorrelation function of the electronic wave packet is calculated when a short laser pulse is applied to the system. With an increase in the laser pulse width, the height and width of the peak in the autocorrelation function increase, but the number of peaks decreases. New recurrences appear because of the interaction between the electron and the helium surface, and the number of recurrent peaks increases with a decrease in the atom-surface distance. The new feature can be ascribed to the bifurcation of new closed orbits in the classical dynamics of the photoionized electron. These new features should be tested in future experiments.

This work was partially supported by the State Key Development Program of the Basic Research of China (No. 2007CB310405), the National Natural Science Foundation of China (No. 10974146), and the Zhejiang Provincial Natural Science Foundation (No. Y6090222).

References

1. A. ten Wolde, L. D. Noordam, A. Lagendijk, and H. B. van Linden van den Heuvell, Phys. Rev. A **40,** 485 (1989).
2. M.-L. Du, Commun. Theor. Phys. **39,** 705 (2003).
3. S. Lin, H. Li, D. Wang, W. Zhao, and F. Gao, Sci. China Ser. G Phys. Mech. Astron. **47,** 477 (2006).
4. L. Wang, Y. Wang, S. Ran, and G. Yang, J. Electron. Spectrosc. Relat. Phenom. **173,** 40 (2009).
5. L. Wang and G. Yang, Chin. Opt. Lett. **7,** 1 (2009).
6. L. Fronzoni, M. Giocondo, and M. Pettini, Phys. Rev. A **43,** 6483 (1991).
7. M. L. Du and J. B. Delos, Phys. Rev. Lett. **58,** 1731 (1987).
8. M. L. Du and J. B. Delos, Phys. Rev. A **38,** 1896 (1988).
9. M. L. Du and J. B. Delos, Phys. Rev. A **38,** 1913 (1988).
10. G. Yang, Y. Zheng, and X. Chi, Phys. Rev. A **73,** 043413 (2006).
11. G. Yang, Y. Zheng, and X. Chi, J. Phys. B: At. Mol. Opt. Phys. **39,** 1855 (2006).
12. L. Wang, Y. Wang, S. Ran, and G. Yang, J. Chem. Phys. **130,** 174706 (2009).
13. Y. P. Zhang, C. H. Cheng, J. T. Kim, J. Stanojevic, and E. E. Eyler, Phys. Rev. Lett. **92,** 203003 (2004).
14. D. Wang, Chin. Opt. Lett. **8,** 553 (2010).
15. J. Gao, J. B. Delos, and M. Baruch, Phys. Rev. A **46,** 1449 (1992).
16. M. L. Du, Phys. Rev. A **51,** 1955 (1995).
17. J. Gao and J. B. Delos, Phys. Rev. A **46,** 1455 (1992).
18. J. Gao and J. B. Delos, Phys. Rev. A **49,** 869 (1994).